2016

The effect of viscous force on the prediction of muscle contractility in biohybrid cantilever-based experiments

Bahador Marzban
University of Rhode Island

Hongyan Yuan
University of Rhode Island, hongyan_yuan@uri.edu

Citation/Publisher Attribution
Marzban, B., & Yuan, H. (2016). The effect of viscous force on the prediction of muscle contractility in biohybrid cantilever-based experiments. *Extreme Mechanics Letters, 9*, Part 2, 342-346. doi: 10.1016/j.eml.2016.09.011
Available at: https://doi.org/10.1016/j.eml.2016.09.011

The effect of viscous force on the prediction of muscle contractility in biohybrid cantilever-based experiments

Bahador Marzban, Hongyan Yuan*

Department of Mechanical, Industrial & Systems Engineering, University of Rhode Island, Kingston, RI 02881 USA

*Corresponding Author:

Hongyan Yuan
Department of Mechanical, Industrial & Systems Engineering
92 Upper College Road
Kingston, RI 02881
Phone: 401-874-2774
Fax: 401-874-2355
Email: hongyan_yuan@uri.edu

Abstract:

The biohybrid cantilevers have been recently reported for high-throughput measurement of muscle contractility. In previous works, mechanical models were used to predict the contractile stress from the cantilever bending curvature. To derive those models, the cantilever bending process was considered as quasi-static and the viscous force was neglected. To ascertain the effect of the viscous force on the prediction of the muscle contractility in biohybrid cantilever-based experiments, we extend the modified Stoney's equation to a dynamic model that takes into account both the viscous force and the inertia force. Parametric studies show that, because the viscous force hinders the movement of the cantilever, use of static models result in a system error between the calculated and true contractile stresses. When using static models, the diastolic stress will be over-estimated while the peak systolic stress will be under-estimated. The present work suggests that dynamic models can be used in biohybrid cantilever assays to calculate the muscle contractility with higher accuracy, or can be used to optimize the experimental parameters such that the error due to the use of static models is minimized.

Keywords: Biohybrid cantilever, Muscle on chips, Stoney's equation, Viscosity

1. Introduction

Important progresses in developing biohybrid cantilever devices for the measurement of muscle contractility have been reported recently [1–9]. In the biohybrid cantilever devices, muscle cells are cultured on the top of a thin substrate layer that can be made of polymers, hydrogels, or silicon. Paced by electric stimulation, the muscle tissue undergoes the cycles of contraction and relaxation, causing the cantilever to bend and recoil periodically (Fig. 1). These types of biohybrid cantilever micro-systems can be used as mechanical sensors for measuring muscle contractility. The contractility of muscle tissue is an important physiological property of muscle tissues, and the high-throughput assays for measuring muscle contractility are an unmet need for biomedical applications such as drug discovery and safety [2,4] and disease modeling [10].

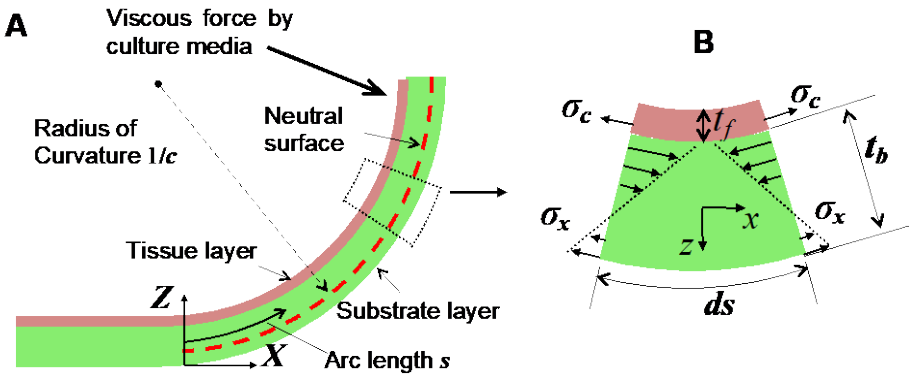

Figure 1. Schematic of the bending movement of the biohybrid cantilever. (A) Side view of the biohybrid cantilever. (B) The stress distribution σ_x on the cross-section of a differential element of the cantilever.

By measuring the deflection of the cantilever and with given geometric and material properties of the cantilever and tissue, the contractile stress of the muscle tissue can be estimated by using mechanics models. When the curvature of the cantilever is assumed to be constant longitudinally, a modified Stoney's equation has been used in the literature [5,7,8,10] to calculate the contractile stress σ_c from the constant curvature c (see the derivations in Model Description):

$$\sigma_c = \bar{E}\frac{{t_b}^2}{6t_f}\frac{1}{(1+t_f/t_b)}c \qquad (1)$$

where t_b is the thickness of the substrate layer, t_f is the thickness of the muscle sheet, the factor $\left(1 + t_f/t_b\right)^{-1}$ is a correction to the original Stoney's equation when the thickness of the muscle layer approaches that of the cantilever beam. Here $\bar{E}$ is an elastic modulus of the cantilever beam that will be clarified as follows. In the original Stoney's equation [11], the effect of cantilever width is ignored and $\bar{E}$ is simply equal to the Young's modulus E. When the cantilever is considered as a thin plate and the muscle sheet develops isotropic contraction [7,8], $\bar{E}$ is taken to be the biaxial modulus $E/(1-v)$, where v is the Poisson's ratio of the substrate layer. In the recently reported muscle-on-a-chip assays [4], the anisotropic muscle cell alignment was achieved by micro-patterning of extracellular matrix proteins on the surface of the cantilever. The muscle sheet developed unidirectional contraction along the length direction of the cantilever. In this case, following the plate theory of cylindrical bending the uniaxial modulus $E/(1-v^2)$ should be used for $\bar{E}$.

It is worth noting that finite element models have also been developed to predict the large deformations of the muscular thin films under the active muscle contraction [4,12,13]. In the muscular thin films, the two-layer biohybrid constructs can have much more complex geometries and tissue alignments than the cantilever counterparts. Böl et al. [12] developed a finite element model of muscular thin films in which the active contraction of the muscle fibers was modeled using 3D truss elements and the polymeric thin film was modeled using the tetrahedral unit cell. In another work, Shim et al. [13] developed a constitutive law of muscle tissue that takes into account the anisotropic pre-stretch and active contraction of muscle fibers. Thanks to the ability to model the complex geometries and material properties with the high accuracy, finite element models are very useful in designing complex muscle-based biohybrid devices [5,14].

Previous analytical and computational modeling of biohybrid cantilevers or muscular thin films have been mainly focused on the static equilibrium of the biohybrid constructs. In these studies, the cantilever is assumed to be in a static equilibrium at any time instant under the acting of the muscle contractile force and the elastic recoiling force of the cantilever itself. However, there has been little effort to date to study the effect of viscous force on the motion of the biohybrid cantilevers. Because the cantilever is immersed in the cell culture media, viscous drag is also

applied on the cantilever when it undergoes dynamic bending-recoiling process. Considering the bending movement of the biohybrid cantilever as a vibration problem, the input is muscle contractile stress and the output is the cantilever deformation (e.g., curvature). For a forced vibration system with damping, the damping force can change both the amplitude and phase of the output. To ascertain the effect of the viscous force on the prediction of the contractility using biohybrid cantilever systems, in the present work, we extend the Stoney's equation to a dynamic model that takes into account both the viscous force and the inertia force.

2. Model Description

The Lagrangian mechanics is applied here to derive the dynamic equation of motion of the cantilever. In the following, we first derive the elastic bending energy of the beam, the potential function of the active contraction, the dissipative function of the viscous force, and the kinetic energy of the beam. We then apply Lagrangian mechanics to derive the dynamic equations.

The model developed below is for the anisotropic muscle tissue [4], i.e., the contraction is unidirectional along the longitudinal direction, which leads to a cylindrical bending of the cantilever. By virtue of the small thickness-to-length ratio, the cantilever is treated using the classic plate theory. To make the model analytically tractable, the curvature along the length of the cantilever is assumed to be constant. Adopting the plain-strain assumption along the width direction of the cantilever, for the cylindrical bending of plates, the normal stress σ_x on the cross-section of the substrate layer in the local coordinates (Fig. 1B) is related to the strain ε_x as [15]:

$$\sigma_x = \bar{E}\varepsilon_x \qquad (2)$$

where $\bar{E} = E/(1-v^2)$ is the uniaxial modulus. Here the normal strain $\varepsilon_x(z)$ can be obtained from the curvature c by: $\varepsilon_x(z) = c(z-b)$, where z measures the distance from the middle layer of the substrate (Fig. 1B), b denotes the position of the neutral axis. The bending strain energy V_b can be calculated as

$$V_b = LW\int_{-\frac{t_b}{2}}^{\frac{t_b}{2}} \frac{1}{2}\sigma_x\varepsilon_x dz \qquad (3)$$

where W and L are the width and length of the cantilever, respectively. Substituting Eq. (2) into Eq. (3), we obtain:

$$V_b = \frac{\bar{E}LW{t_b}^3}{24}c^2 + \frac{\bar{E}LWt_b}{2}c^2b^2 \qquad (4)$$

The elastic bending energy of the tissue layer can be neglected because the Young's modulus of the muscle tissue is at least two orders of magnitude smaller than the cantilever that is made of polymer or silicon. For the hydrogel cantilevers [16], the thickness of the cantilever is much larger than the tissue layer. In both cases, the bending rigidity of the cantilever is much larger than the muscle layer, which justifies ignoring of the bending strain energy of the muscle layer. Using the strain at the middle of tissue layer, the potential function V_c for the cell contraction stress can be calculated as:

$$V_c = \sigma_c LW t_f c\left(-\frac{t_f+t_b}{2} - b\right) \qquad (5)$$

To calculate the kinetic energy, the velocity of the cantilever is estimated as follows. In the global coordinate system, defining $X(s)$ and $Z(s)$ as the current configuration of the beam, where s is the arc length, one have $X(s) = \int_0^s coscs'ds' = \frac{1}{c}sincs \sim s - \frac{s^3}{6}c^2$, and $Z(s) = \int_0^s sincs'ds' = \frac{1}{c}(1-coscs) \sim \frac{s^2}{2}c$. Taking derivative of $X(s)$ and $Z(s)$ with respect to time, the magnitude of the velocity $\bar{v}(s)$ of the cantilever as a function of the arc length s can be approximated as

$$\bar{v}(s) = \dot{c}\sqrt{\frac{s^6}{9}c^2 + \frac{s^4}{4}} \qquad (6)$$

The kinetic energy E_k of the cantilever can be calculated as $E_k = \frac{\rho t_b W}{2}\int_0^L \bar{v}(s)^2 dx$, where ρ is the density of the substrate material. Using Eq. (6), the kinetic energy can be obtained as follows:

$$E_k = \frac{\rho t_b L^7 W}{126}\dot{c}^2 c^2 + \frac{\rho t_b L^5 W}{40}\dot{c}^2 \qquad (7)$$

The viscous force exerted on the cantilever is taken into account through a dissipation function V_d in an integral form,

$$V_d = \frac{\alpha\mu}{2}\int_0^L \bar{v}(s)^2 ds \qquad (8)$$

where α is a dimensionless number and μ is the dynamic viscosity of the culture media. To be analytical tractable, α will be estimated here in an ad hoc approach. The dimensionless number involved in the calculation of viscous force for a plate with a width W and a length L moving in a viscous fluid is given [17] as $\alpha = 6\pi(3W + 2L)/5L$. This formula is used here for the estimation of the numerical value of α. Substituting velocity from Eq. (6) into equation Eq. (8), we derive the dissipation function V_d as

$$V_d = \frac{\alpha\mu L^7}{126}\dot{c}^2 c^2 + \frac{\alpha\mu L^5}{40}\dot{c}^2 \qquad (9)$$

The Lagrangian $\mathcal{L}$ can be calculated as follows:

$$\mathcal{L} = E_k - (V_b + V_c) \qquad (10)$$

Recall that the general form of the Lagrange's equation for a system with two generalized coordinates (i.e., b and c) takes the following form:

$$\frac{d}{dt}\frac{\partial \mathcal{L}}{\partial \dot{b}} - \frac{\partial \mathcal{L}}{\partial b} = -\frac{\partial V_d}{\partial \dot{b}} \qquad (11)$$

$$\frac{d}{dt}\frac{\partial \mathcal{L}}{\partial \dot{c}} - \frac{\partial \mathcal{L}}{\partial c} = -\frac{\partial V_d}{\partial \dot{c}} \qquad (12)$$

Since the Lagrangian $\mathcal{L}$ is independent of the $\dot{b}$, Eq. (11) can be simplified to:

$$b = \frac{\sigma_c t_f}{\bar{E} t_b}\frac{1}{c} \qquad (13)$$

By substituting Eq. (10) and (13) into Eq. (12), the general governing equation of motion for this dynamic model is obtained:

$$\left(\frac{\rho t_b L^5 W}{20} + \frac{\rho t_b L^7 W}{63}c^2\right)\ddot{c} + \left(\frac{\alpha\mu L^5}{20} + \frac{\alpha\mu L^7}{63}c^2\right)\dot{c} + \left(\frac{\bar{E}{t_b}^3 LW}{12} + \frac{\rho t_b L^7 W}{63}\dot{c}^2\right)c = \frac{(t_b+t_f)t_f LW}{2}\sigma_c(t) \qquad (14)$$

In the case of cantilever bending in the small curvature and slow motion region, by neglecting the nonlinear terms in equation (14), the linear equation of motion can be obtained in the following form:

$$\frac{\rho t_b L^4}{10(t_b+t_f)t_f}\ddot{c} + \frac{\alpha\mu L^4}{10(t_b+t_f)t_f W}\dot{c} + \frac{\bar{E}{t_b}^2}{6(1+t_f/t_b)t_f}c = \sigma_c(t) \qquad (15)$$

If neglecting the viscous and inertia forces, i.e., by setting $\dot{c} = 0$ and $\ddot{c} = 0$ in Eq. (15), we recover the modified Stoney's equation given in Eq. (1). Equation (15) indicates that because of the presence of viscous and inertia force on the cantilever, the muscle contractility σ_c is not simply proportional to the curvature c, but a function of c and its time derivatives. Therefore, using the Stoney's equation or its variants in the contractility measurement assays will result in a system error.

To show quantitatively how the bending motion of the cantilever is affected by the viscous force, Eq. (14) and (15) are solved numerically with an assumed function $\sigma_c(t)$. We assume the calcium-induced muscle contractile stress $\sigma_c(t)$ is decoupled from the bending of the cantilever, and in one period it is described as

$$\sigma_c(t) = \begin{cases} (\sigma_{sy} - \sigma_{di})\left[\frac{1-cos\left(\frac{2\pi}{t_c}t\right)}{2}\right] + \sigma_{di}, & 0 \le t \le t_c \\ \sigma_{di}, & t_c < t < T \end{cases} \qquad (16)$$

where σ_{sy} and σ_{di} are peak systolic and diastolic stresses, respectively, t_c is the twitch period, T is the pacing period. Thus, the pacing frequency is $1/T$. With $\sigma_c(t)$ as the given input, the curvature $c(t)$ as a function of time can be obtained from Eq. (14) or (15). In the results presented below, parameters values are estimated from previous experiments [10]: μ =0.001 Pa·s, t_f = 4 μm, t_b = 20 μm, L = 4 mm, W = 2mm, α = 13.2, σ_{sy} = 20 kPa, σ_{di} = 8 kPa, ν = 0.5, E = 1.52 MPa, ρ = 965 kg/m^3. These values are used in all of the calculations unless specifically mentioned.

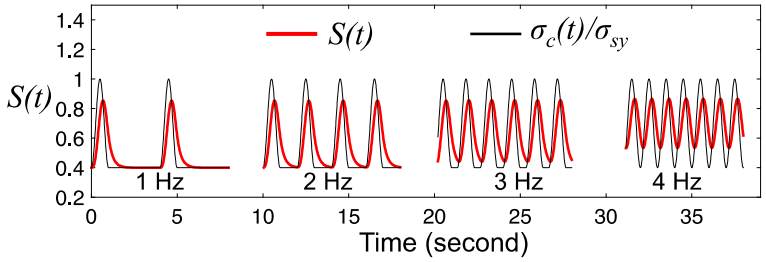

Figure 2. Effect of pacing frequency on the dynamics of cantilever bending. The bending curvature is represented by the dimensionless quantity $S(t)$. The thinner line represents the normalized contractile stress. The thicker line is the steady-state solution from the linear dynamic model (Eq. (15)).

Results

The significance of viscous and inertia forces to the cantilever bending movement can be estimated by the following order-of-magnitude analysis. By using the approximation $\ddot{c}/c \sim {t_c}^{-2}$, the ratio between the inertia force and the elastic recoiling force can be estimated as

$$\varsigma = \frac{(3\rho t_b L^5 W)\ddot{c}}{(5\bar{E} {t_b}^3 LW)c} \sim \frac{\rho L^4}{\bar{E} {t_b}^2 {t_c}^2} \qquad (17)$$

For the experimentally relevant parameter values (listed in the caption of Fig. 2), the ratio ς is calculated to be 0.005, which is two orders of magnitude smaller than one. The ratio between the viscous force and the elastic recoiling force can be estimated as

$$\chi = \frac{(3L^5 \alpha\mu)\dot{c}}{(5\bar{E} {t_b}^3 LW)c} \sim \frac{\alpha\mu L^4}{\bar{E} {t_b}^3 W t_c} \qquad (18)$$

For the same set of parameter values, the ratio χ is found to be 0.4, which is close to 1. These order-of-magnitude analyses indicate that, compared to the elastic recoiling force, the viscous force is comparable to the elastic recoiling force, while the inertia force is negligible.

To facilitate the discussion of the modeling results, we introduce a dimensionless quantity $S(t) = \frac{1}{\sigma_{sy}} \frac{\bar{E} {t_b}^2}{6(1+t_f/t_b)t_f} c(t)$ by dividing the left-hand side of Eq. (15) by the peak systolic stress σ_{sy}. Note that $S(t)$ can be interpreted as the scaled curvature and it can also be interpreted as the predicted contractile stress from the curvature when using the modified Stoney's equation (Eq. (1)). The steady state solution of Eq. (15) (i.e., the linear dynamic model) is plotted in Fig. 2, in which the dimensionless quantity $S(t)$ and the normalized contractile stress $\sigma_c(t)/\sigma_{sy}$ are plotted. The solutions for different pacing frequencies (1 Hz, 2 Hz, 3 Hz, and 4 Hz) are placed together in the time domain for the ease of comparison. For the steady state solution $S(t)$ at each frequency, we denote the maximal and minimal values by S_{max} and S_{min}, respectively. The true maximal and minimal contractile stress is defined by the peak systolic stress σ_{sy} and the diastolic stress σ_{di}, respectively. We can see from Fig. 2 that $S_{min} \geq \sigma_{di}$ while $S_{max} \leq \sigma_{sy}$. Therefore, in the previous experiments when using the static models such as the modified Stoney's equations to predict the contractile stress, the diastolic stress will be over-estimated, while the peak systolic stress will be under-estimated. Mechanically, these results can be interpreted as follows. For $S_{max} \leq \sigma_{sy}$, it is because when the muscle tissue contracts to bend the cantilever, the cantilever only bends to a less extent (compared to a static equilibrium case) due to the viscous force. For $S_{min} \geq \sigma_{di}$, at the end of the elastic recoiling, for sufficiently high pacing frequency, the next contraction cycle starts before the cantilever recoils all the way to the lowest position in a static situation. In addition, there is also a slight phase shift between the input (contractile stress) and the output (the curvature), as shown in Fig. 2.

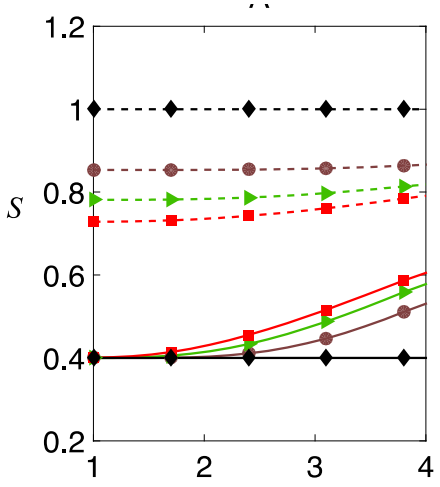

in ,

Figure 3. Effects of the dynamic viscosity μ on S_{min} and S_{max}. (A) Solutions of the linear dynamic model (Eq. (15)). (B) Solution of the nonlinear dynamic model (Eq. (14)). Both panel A and B share the same legend.

Figure 3 plots S_{max} and S_{min} as functions of the pacing frequency for different values of viscosity and for the linear and nonlinear dynamic models. The upper bound of the pacing frequency in x-axis is set to be $1/t_c$, which is the maximal pacing frequency at which there is no overlap between the adjacent contraction-relaxation cycles. It can be seen that, both S_{min} and S_{max} increase with the increasing of the pacing frequency. This is because the faster the pacing frequency, the earlier the next contraction starts, yielding larger S_{min}. At faster pacing frequency, the increase of S_{min} yields a higher starting position for the next contraction cycle, thus increasing S_{max}. Denoting the difference between S_{max} and S_{min} by ΔS_{tw} (i.e., $\Delta S_{tw} = S_{max} - S_{min}$), ΔS_{tw} is shown to decrease with increasing the pacing frequency, which is because the increase of S_{min} outnumbers the increase of S_{max}. Furthermore, Fig. 3 shows as the viscosity becomes larger, the difference between S_{min} and σ_{di} becomes greater. This is also the case for the difference between S_{max} and σ_{sy}. Because $(S_{min} - \sigma_{di})$ and $\left(S_{max} - \sigma_{sy}\right)$ represent the system error when the static models are used to predict the contractile stress from the curvature, we see that the system error increases with the viscosity of the culture media. Comparing the results of the nonlinear dynamic model (Fig. 3B) with the linear one (Fig. 3A), in the nonlinear

case the effect of the viscous force on deviating S_{max} and S_{min} from σ_{sy} and σ_{di}, respectively, is even larger.

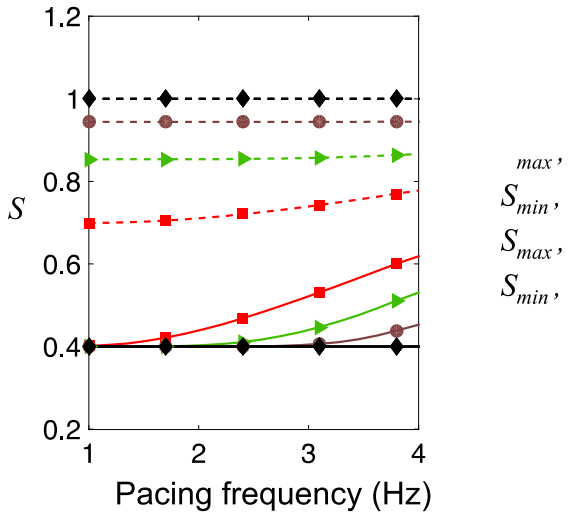

Figure 4. Effect of the thickness of the substrate layer t_b on S_{min} and S_{max}, the linear dynamic model is used for the calculations.

From the scale analysis in Eq. (18), the ratio between the viscous force and the elastic recoiling force can be tuned by changing the thickness of the substrate layer. Figure 4 plots S_{max} and S_{min} as functions of the pacing frequency for different thicknesses of the substrate layer, in which one can see that both $(S_{min} - \sigma_{di})$ and $\left(S_{max} - \sigma_{sy}\right)$ decrease with increasing of the thickness t_b. This is simply because increasing the thickness of the substrate layer will decrease the ratio χ between the viscous force and the elastic recoiling force (Eq. (18)), thus decreasing the system error when the static models are used to predict the contractile stress from the curvature. However, increase the thickness of the substrate layer will reduce the signal strength (i.e., decreasing the dynamic range of the bending curvature of the cantilever). Therefore, an optimal thickness of the substrate layer exists, at which the best accuracy of the contractility measurement can be achieved.

Conclusions

In this work, we have developed an analytical model to solve for the relation between the cantilever bending curvature and the muscle contractile stress for the biohybrid cantilever system. Although in the present model, only one layer of flat substrate material is considered, the analytical approach can be readily extended to micro-molded hydrogel cantilevers [16] and multi-layer cantilevers by describing the strain energy of bending in each layer. We have shown that, due to the presence of the viscous force acting on the cantilever, the quasi-static relation between the curvature and the contractile stress (Eq. (1)) is no longer valid and results in a system error between the estimated and true values of muscle contractility. The modeling results show that, for the same muscle tissue, the minimal and maximal curvatures of the cantilever changes with the pacing frequency. When using a static model to calculate the contractile stress from the measured curvature, the calculated diastolic stress will be larger than the true diastolic stress, while the calculated peak systolic stress will be smaller than the true values. The calculated twitch stress will be smaller than the true value. In addition, the error for the diastolic stress is smaller at the lower pacing frequency, while the error for the peak systolic stress is bigger at the lower pacing frequency (Fig. 3). Our work suggests that dynamic models can be used to calculate the muscle contractility with higher accuracy. On the other hand, in the cases where the static models are highly favored in the experiments by virtue of its simplicity and the need of less number of parameters, dynamic models can be used to optimize the parameters such that the error due to the use of the static models is minimized.

References

[1] A. Agarwal, Y. Farouz, A. P. Nesmith, L. F. Deravi, M. L. McCain, and K. K. Parker, *Micropatterning Alginate Substrates for in Vitro Cardiovascular Muscle on a Chip* (2013), pp. 3738–3746.

[2] A. Agarwal, J. A. Goss, A. Cho, M. L. McCain, and K. K. Parker, *Microfluidic Heart on a Chip for Higher Throughput Pharmacological Studies* (2013), pp. 3599–608.

[3] A. P. Nesmith, A. Agarwal, M. L. McCain, and K. K. Parker, *Human Airway Musculature on a Chip: An in Vitro Model of Allergic Asthmatic Bronchoconstriction and Bronchodilation* (Royal Society of Chemistry, 2014), pp. 3925–3936.

[4] A. Grosberg, A. P. Nesmith, J. A. Goss, M. D. Brigham, M. L. McCain, and K. K. Parker, *Muscle on a Chip: In Vitro Contractility Assays for Smooth and Striated Muscle* (Elsevier Inc., 2012), pp. 126–135.

[5] A. W. Feinberg, A. Feigel, S. S. Shevkoplyas, S. Sheehy, G. M. Whitesides, and K. K. Parker, *Muscular Thin Films for Building Actuators and Powering Devices* (2007), pp. 1366–70.

[6] J. Xi, J. J. Schmidt, and C. D. Montemagno, *Self-Assembled Microdevices Driven by Muscle* (Nature Publishing Group, 2005), pp. 180–184.

[7] K. Wilson, M. Das, K. J. Wahl, R. J. Colton, and J. Hickman, *Measurement of Contractile Stress Generated by Cultured Rat Muscle on Silicon Cantilevers for Toxin Detection and Muscle Performance Enhancement* (2010).

[8] V. Chan, J. H. Jeong, P. Bajaj, M. B. Collens, T. A. Saif, H. Kong, and R. Bashir, *Multi-Material Bio-Fabrication of Hydrogel Cantilevers and Actuators with Stereolithography* (2012), pp. 88–98.

[9] L. Ricotti and A. Menciassi, *Bio-Hybrid Muscle Cell-Based Actuators* (2012), pp. 987–998.

[10] G. Wang, M. L. McCain, L. Yang, A. He, F. S. Pasqualini, A. Agarwal, H. Yuan, D. Jiang, D. Zhang, L. Zangi, J. Geva, A. E. Roberts, Q. Ma, J. Ding, J. Chen, D.-Z. Wang, K. Li, J. Wang, R. J. A. Wanders, W. Kulik, F. M. Vaz, M. A. Laflamme, C. E. Murry, K. R. Chien, R. I. Kelley, G. M. Church, K. K. Parker, and W. T. Pu, *Modeling the Mitochondrial Cardiomyopathy of Barth Syndrome with Induced Pluripotent Stem Cell and Heart-on-Chip Technologies* (Nature Publishing Group, a division of Macmillan Publishers Limited. All Rights Reserved., 2014), pp. 616–23.

[11] C. A. Klein, *How Accurate Are Stoney's Equation and Recent Modifications* (2000), p. 5487.

[12] M. Böl, S. Reese, K. K. Parker, and E. Kuhl, *Computational Modeling of Muscular Thin Films for Cardiac Repair* (2009), pp. 535–544.

[13] J. Shim, A. Grosberg, J. C. Nawroth, K. Kit Parker, and K. Bertoldi, *Modeling of Cardiac Muscle Thin Films: Pre-Stretch, Passive and Active Behavior* (Elsevier, 2012), pp. 832–841.

[14] S.-J. Park, M. Gazzola, K. S. Park, S. Park, V. Di Santo, E. L. Blevins, J. U. Lind, P. H. Campbell, S. Dauth, A. K. Capulli, F. S. Pasqualini, S. Ahn, A. Cho, H. Yuan, B. M. Maoz, R. Vijaykumar, J.-W. Choi, K. Deisseroth, G. V. Lauder, L. Mahadevan, and K. K. Parker, *Phototactic Guidance of a Tissue-Engineered Soft-Robotic Ray* (2016), pp. 158–162.

[15] S. Timoshenko and S. Woinosky-Krieger, *Theory of Plates and Shells Classic* (1959).

[16] M. L. McCain, A. Agarwal, H. W. Nesmith, A. P. Nesmith, and K. K. Parker, *Micromolded Gelatin Hydrogels for Extended Culture of Engineered Cardiac Tissues* (Elsevier Ltd, 2014), pp. 5462–5471.

[17] F. M. White, *Viscous Fluid Flow*, 2nd ed. (McGraw-Hill, 1991).